Analytical Methods

Accepted Manuscript

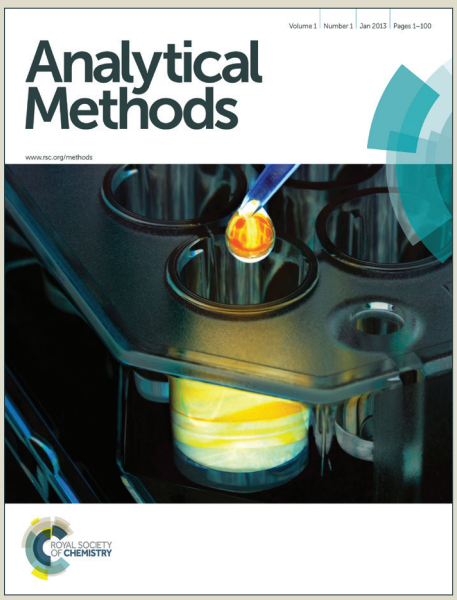

ROYAL SOCIETY OF CHEMISTRY

www.rsc.org/methods

Eelectrochemical sensor for paracetamol based on electropolymerized molecularly imprinted *o*-phenylenediamine film on a multi-walled carbon nanotube modified glassy carbon electrode

Youyuan Peng*, Zhibo Wu, Zhigang Liu

Department of Chemistry, Quanzhou Normal University, Quanzhou 362000, China

Abstract: An electrochemical sensor combining molecular imprinted technique and electropolymerization method was developed in this work. A molecular imprinted polymer film was fabricated by electropolymerizing *o*-phenylenediamine in the presence of paracetamol after depositing carboxylfunctionalized multi-walled carbon nanotubes onto a glassy carbon electrode surface. The template can be quickly removed in 50% ethanol. The molecularly imprinted sensor was tested in the presence or absence of paracetamol by cyclic voltammetry and linear sweep voltammetry to characterize the constructed sensor. The molecular imprinted polymer based sensor displayed an excellent recognition capacity toward paracetamol compared with other structurally similar molecules. Additionally, the linear sweep voltammetry peak current was linear to the concentration of the analyte in the range from 2.0×10^{-7} to 4.0×10^{-5} mol L^{-1}, with a detection limit of 5.0×10^{-8} mol L^{-1}. The prepared sensor also showed stable repeatability and regeneration capacity. The sensor was applied to the determination of paracetamol in real samples successfully, with the recoveries ranging from 94% to 105%.

Keywords: Multi-walled carbon nanotubes; Molecular imprinting technique; Paracetamol; Electrochemical polymerization

Introduction

Paracetamol (acetaminophen, N-acetylp-aminophenol) is widely used as an antipyretic and analgesic drug. Paracetamol (PT) is a long-established and one of the most extensively employed ‘‘over the counter’’ drugs in the world. It is an effective and safe agent that is applied to reduce fever, relieve

* Corresponding author.
E-mail: youyuanpeng@hotmail.com. Fax: 86-595-2291 9563. Tel: 86-595-2291 9563.

coughing, colds, and pain including muscular aches, backache, and toothache.[1-3] Generally, limited use of PT does not exhibit any harmful side effects. However, overdosing and the chronic use of PT produce toxic metabolite accumulation that will cause kidney and liver damage.[4] The large scale therapeutic use of this drug generated the need for the development of fast, simple and accurate methodologies for the detection of PT; for quality control analysis (in pharmaceutical formulations) and for medical control (in biological fluids such as urine, blood and plasma).[5,6]

Several methods have been used for the determination of PT in pharmaceutical formulations and biological fluids, including spectrophotometry,[7] flow-injection[8] and chromatographic methods.[9] Although these methods are sensitive and highly reliable, they often require time consuming complex pretreatment steps and the apparatus and operating cost are expensive for routine analysis. Electrochemical detection is an attractive method due to its simplicity, low expense and high sensitivity, several reports have been published recently for the determination of PT by using electrochemical sensors.[10-14]

Recently, the interest in sensors based on molecularly imprinted polymer (MIP)[15,16] has grown remarkably, probably owing to its predetermined selectivity and recognition ability for target molecules. This technique is based on the co-polymerization of functional monomers and cross-linking monomers in the presence of the molecular template. After co-polymerization, the functional groups are “frozen” in the cross-linked polymeric network. Subsequent removal of the template molecule leads to empty cavities in the polymer structure, which are complementary in size, shape and functionality to the template. The MIP thus has a molecular memory and is able to specifically recognize and rebind the template molecule.[17] Among many methods for MIP preparation, electropolymerization is a potential technique for developing electrochemical sensors and can deposit a recognition film with spatial selectivity on the detector surface with no restriction to the choice of the analyte.[18-20] Electropolymerization allows for the generation of a rigid, uniform, and compact MIPs film with good adherence onto an electrode surface of any shape and size.[21-23] Moreover, the thickness and density of the film is adjustable by controlling polymerization conditions. Therefore, many MIP-based sensors have been prepared and used to recognize and detect different

molecules.[24-26] With unique properties at the nanoscale dimension for enhancing the sensitivity of the electrochemical detection, multiwalled carbon nanotubes (MWCNTs) have been used for molecular imprinting.[15,16,27,28]

To our knowledge, no studies were reported on the application of MWCNTs-MIP film modified electrodes for the detection of PT up to now. In this study, a novel kind of MIP-based electrochemical sensor was fabricated successively by depositing carboxylfunctionalized MWCNTs (MWCNTs-COOH) and electropolymerizing *o*-phenylenediamine (*o*PD) in the presence of PT onto a glassy carbon electrode (GCE) surface. Because *o*PD has been proven to be easily electropolymerized on various materials to form a nonconductive polymer film in neutral pH with good chemical and mechanical stability,[29,30] it was chosen as functional monomer of electropolymerization in this work. An electroactive substance, potassium ferricyanide, was used as the redox probe of the imprinted film modified electrode in solutions containing the analyte. The prepared sensor was characterized by scanning cyclic voltammetry (CV) and linear sweep voltammetry (LSV). Dopamine (DA), phenacetin (PA), ascorbic acid (AA), adrenaline (AD), and noradrenaline (NAD) were selected as the structurally similar molecules to evaluate the recognition capacity of the prepared sensor. Under the optimized conditions, the sensor exhibited good adsorption and a high recognition capacity for PT. In addition, the analytical performance of this sensor for determination of PT in human serum, human urine and in actual pharmaceutical preparation samples is evaluated.

Experimental details

Chemicals and reagents

Multi-walled carbon nanotubes (MWCNTs) with diameters of 10–30 nm and lengths of 1–2 μm were obtained from Shenzhen Nanotech Port Co. Ltd., China. PT (≥98%) was purchased from National Institutes for Food and Drug Control (Beijing, China). Dopamine (DA), phenacetin (PA), ascorbic acid (AA), adrenaline (AD), noradrenaline (NAD), *o*PD and *N*,*N*-Dimethylformamide (DMF) were

purchased from Sigma-Aldrich. A 0.05 mol L^{-1} phosphate buffer at pH 7.0 was prepared from KH_2PO_4 and $K_2HPO_4 \cdot 3H_2O$ in an appropriate proportion. All other reagents were of at least analytical reagent grade, and double-distilled water was used for all solutions.

Fresh human serum samples were obtained from the 180th Hospital (Quanzhou, China). The serum and urine sample were filtered and diluted 100 times with 0.05 mol L^{-1} PBS of pH 7.0 and checked for the determination of the recovery by spiking with PT.

Preparation of carboxylic acid-functionalized MWCNTs (MWCNTs-COOH)

Received MWCNTs (1 g) were added to 100 mL of 68 % HNO_3 under sonication for 30 min, followed by refluxing at 120 ℃ for 4 hours. After cooling to room temperature, the reaction mixture was then diluted with water and allowed to stand overnight for precipitation. The supernatant was decanted, and the remains were filtered through a 0.22 μm polytetrafluoroethylene membrane and washed thoroughly with distilled water for several times until the pH value of the filtrate was neutral. The solid powders were dried at 70 ℃ under vacuum, obtaining carboxylic acid functionalized MWCNTs (MWCNTs-COOH).

Preparation of modified glassy carbon electrode (MGCE)

Prior to modification, the surface of the bare GCE was carefully hand-polished with a 0.3 and 0.05 μm alumina–water slurry using a polishing cloth in sequence, and thoroughly ultrasonically rinsed with ethanol, and doubly distilled water for 5 min in turn. Then the electrode potential was cycled between −0.50 and +2.00 V in 0.5 mol L^{-1} H_2SO_4 at 100 mV s^{-1} until a stable cyclic voltammogram was obtained. Prior to the deposition of MWCNTs-COOH, the bare GCE was cyclic potential scanned in the potential range from 0.00 to +0.80 V in 1 mmol L^{-1} $K_3[Fe(CN)_6]$ solution containing 0.1 mol L^{-1} KCl supporting electrolyte until a pair of well-defined redox peaks was observed.

A suspension of MWCNTs-COOH (1 mg mL^{-1}) in DMF was prepared by the dispersion of

MWCNTs-COOH using ultrasonic churning. The MWCNTs-COOH layer was modified onto the electrode surface by a traditional dropping method. Small amount (9 μL) of this suspension was put on the surface of bare polished GCE. It was seen that the suspension covered total surface area of the GCE. The suspension was allowed to desiccate by keeping the electrode in open at room temperature (25 ± 2 ◦C). Within about one hour, the solvent evaporated off leaving a thin layer of MWCNTs-COOH all around the electrode surface. The electrode so obtained is called MGCE.

Preparation of imprinted and non-imprinted film modified electrodes

In this process, electropolymerization was performed for MIP preparation. Briefly, the MGCE modified with *o*PD film containing PT was prepared by 20 cycles of cyclic voltammetric measurements in the range 0.00 – +0.80 V (scan rate 50 mV s^{-1}) in phosphate buffer (pH 7.0) containing 5 mmol L^{-1} *o*PD, 5 mmol L^{-1} PT. After the electropolymerization, molecularly imprinted polymers modified MGCE (MIP-MGCE) was obtained by placing the resulting modified MGCE in 20 mL 50% ethanol for 20 min to remove PT from the electrode surface. Non-imprinted polymers modified MGCE (NIP-MGCE) was also prepared and treated in exactly the same manner, except for the omission of PT in the electropolymerization process. The NIP-MGCE was treated with the same procedure as the MIP-MGCE to ensure that the effects observed were only due to the imprinting features and not because of the subsequent treatments the electrode underwent.

Electrochemical measurements

Electrochemical experiments, such as cyclic voltammetry (CV) and linear sweep voltammogram (LSV) were performed on a CHI 800C workstation (ChenHua Instruments Co., Shanghai, China) with a conventional three-electrode system. A bare or modified glassy carbon electrode served as the working electrode, and a saturated calomel electrode and a platinum wire electrode were used as the reference and counter electrodes, respectively. Solutions were deaerated (using pre-purified nitrogen)

for 10 min before the electrochemical experiment.

Results and Discussion

FTIR spectra of MWCNTs

FTIR spectra were applied to characterize the structural changes of MWCNTs. The received MWCNTs almost had no IR adsorption bands (Fig. S1). Compared with the IR spectrum of the received MWCNTs, the characteristic peaks of carbonyl and hydroxyl introduced by -COOH, obviously appeared in the spectrum of MWCNTs-COOH. The peaks at 3431 and 1728 cm^{-1} belonged to stretching vibration of O-H and C=O respectively. The peaks at 2922 and 2853 cm^{-1} were contributed by $-CH_3$ and $-CH_2$ on the surface of the MWCNTs-COOH. All these adsorption bands supported that O-H and -COOH were formed in MWCNTs-COOH.

Electropolymerization

With potential scanning between 0.00 V and +0.80 V at a scan rate of 50 mV s^{-1} for 20 cycles, the typical cyclic voltammograms recorded during the electropolymerization of *o*PD and PT on the GCE and MGCE surface are shown in Fig. 1. The formation and growth of the polymer film can be easily seen.

Fig. 1A shows the electropolymerization performed by repeated potential scanning between 0.00 and +0.80 V for *o*PD and PT at bare GCE. As shown in Fig. 1A, an irreversible oxidation peak, appearing at +0.36 V in the first potential scan, decreased quickly in the following potential scans, which is attributed to *o*PD oxidation and reflects a poly-ophenylenediamine (P*o*PD) film was coated on the electrode, restricting the further oxidation of *o*PD.[31] Fig. 1B shows the cyclic voltammogram of polymerization of *o*PD on MGCE. In the first cycle, a broad and irreversible oxidation peak appeared with a peak potential at about 0.34 V, the anodic peak current decrease during potential cycling

becomes more gradual compared with bare GCE. Higher currents are observed on MGCE for *o*PD oxidation, the presence of MWCNTs could increase surface area of the electrode and facilitate the electron transfer between the electrode and the analytes, therefore the enhancements in the corresponding electrochemical oxidation peak currents were observed. Fig. 1C shows the same cyclic scans of copolymerization of *o*PD on MGCE, but this time in the presence of the template. Electropolymeric mechanism of *o*PD is described in detail in the literature.[32-34] There are significant differences in the cyclic voltammograms obtained under the same conditions but without the template, the peak current at about 0.60 V became much more higher, which may attributed to the fact that the oxidation of PT superimposes over the oxidation peak of *o*PD. This oxidation peak indicates that the template is becoming part of the polymeric chain.[18,35] The oxidation peak of PT shifts to more positive potential, which may be attributed to the presence of a part of nonconductive polymer film formed on the electrode surface. When enlarging the potential window to more negative potential, a redox peak was observed (as shown in Fig. S2), which was attributed to the formation of P*o*PD.[31] Because of the polymerization solution was not stirred, the mass transfer was occurred by diffusion controlled process. PT molecules diffuse towards the surface of the MGCE during the electropolymerization process and were trapped into the polymer matrix.

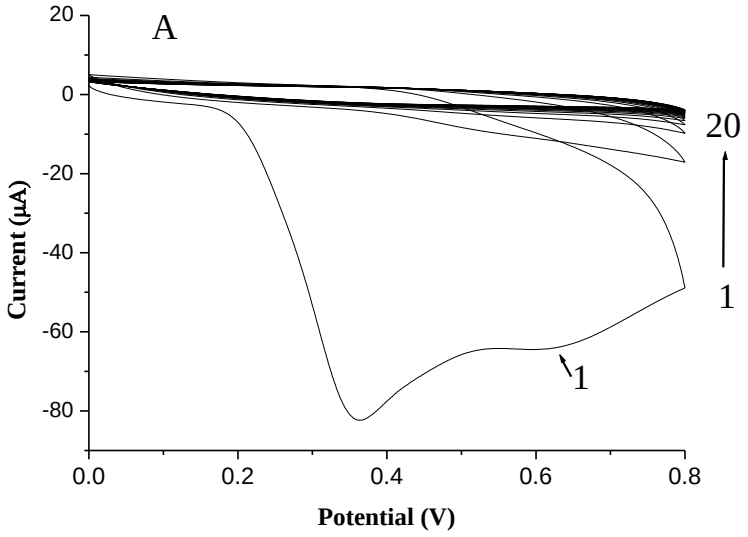

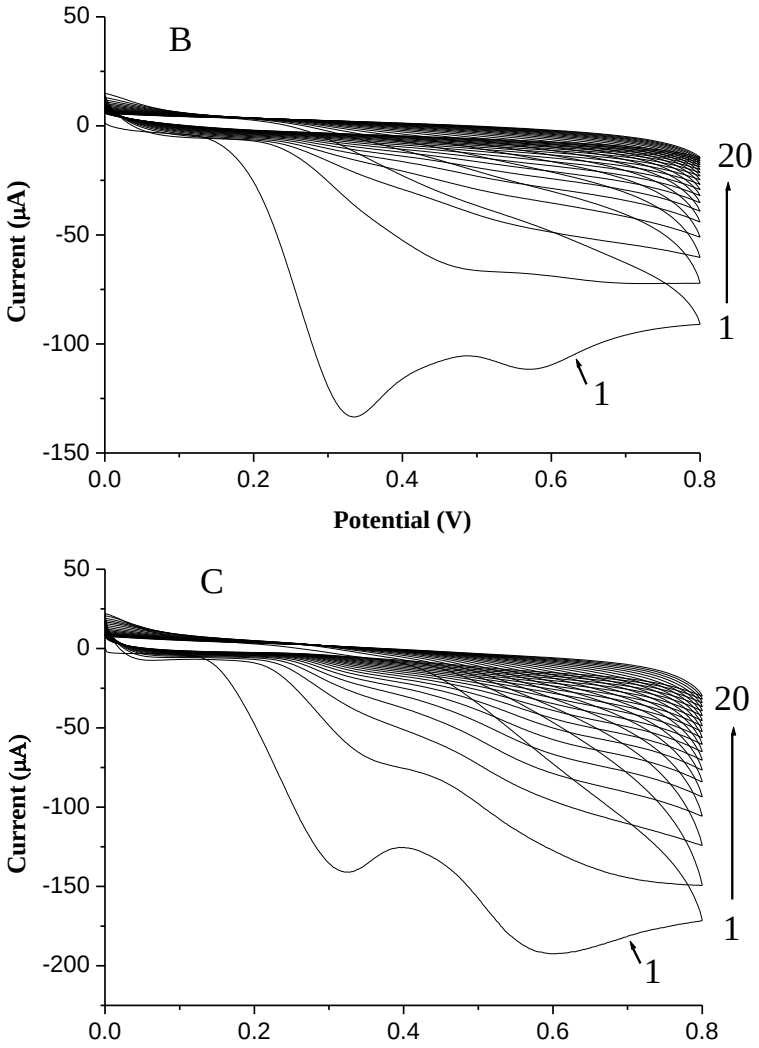

Fig. 1 Repetitive cyclic voltammograms during the electrocopolymerization of *o*PD (5.0 mmol L^{-1}) and PT (5.0 mmol L^{-1}). (A): onto a bare GCE; (B): onto MGCE without PT; (C): onto MGCE. Scan rate: 50 mV s^{-1}. Supporting electrolyte: N_2-saturated PBS (0.05 mol L^{-1}, pH: 7.0) containing 0.1 mol L^{-1} KCl. Scan circles: 20.

FTIR Characterization of MWCNTs/P*o*PD/PT film

The composition of the films was characterized by FTIR spectroscopy. The GCE was ground carefully with KBr crystal after electropolymerization, the spectra of the polymer were recorded using an FTIR Avatar 360 spectrometer (Thermo Nicolet Co., USA). Fig. 2 displays the FTIR spectra of P*o*PD (A), MWCNTs/P*o*PD composite (B) and MWCNTs/P*o*PD/PT composite(C). Fig. 2A shows the

FTIR spectra of the P*o*PD films formed on bare GCE. As shown in Fig. 2A, the broad peak appearing between 3444 and 3132 cm^{-1} represented the absorption band of the N-H stretching vibration of the –NH- group. The peaks at 1622, 1456, and 1162 cm^{-1} were attributed to the C-N, C=C stretching vibrations in the phenazine ring along the polymer chain and the C-N-C stretching in the benzenoid units, respectively.[36] The bands 1400 cm^{-1} confirm the presence of phenazine rings in the P*o*PD backbone.[37,38] Furthermore, peaks at 782 and 572 cm^{-1}**,** which were characteristic of the C-H out of plane bending vibrations in the phenazine ring,[39] were also obtained.

The spectrum of the P*o*PD sample obtained on the MGCE is similar to that of P*o*PD coated on GCE except that there are small shifts in the wavenumbers. The shifts in the wavenumbers, although small, definitely indicate some subtle changes (maybe including hydrogen bond, and π-π interactions between the polymer and MWCNTs) in the structure of the polymer formed on MGCE.

The spectra of the MWCNTs/P*o*PD/PT composite was similar to that of the MWCNTs/P*o*PD composite except for the peaks at 3340, 1642 and 1088 cm^{-1}, the peak at 1642 cm^{-1} was contributed to the stretching vibration of C=O, which existed in the PT molecules. The results suggest that PT was imprinted in P*o*PD film during the electropolymerization of *o*PD in the presence of PT.

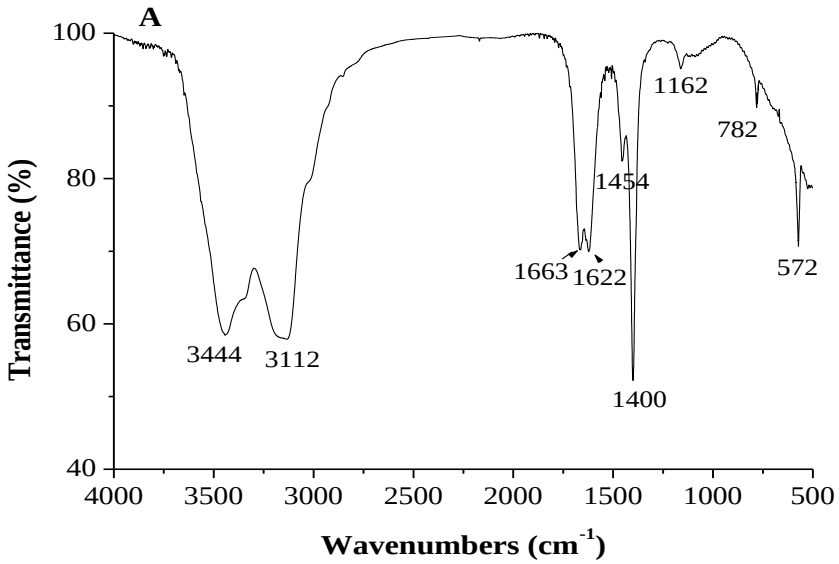

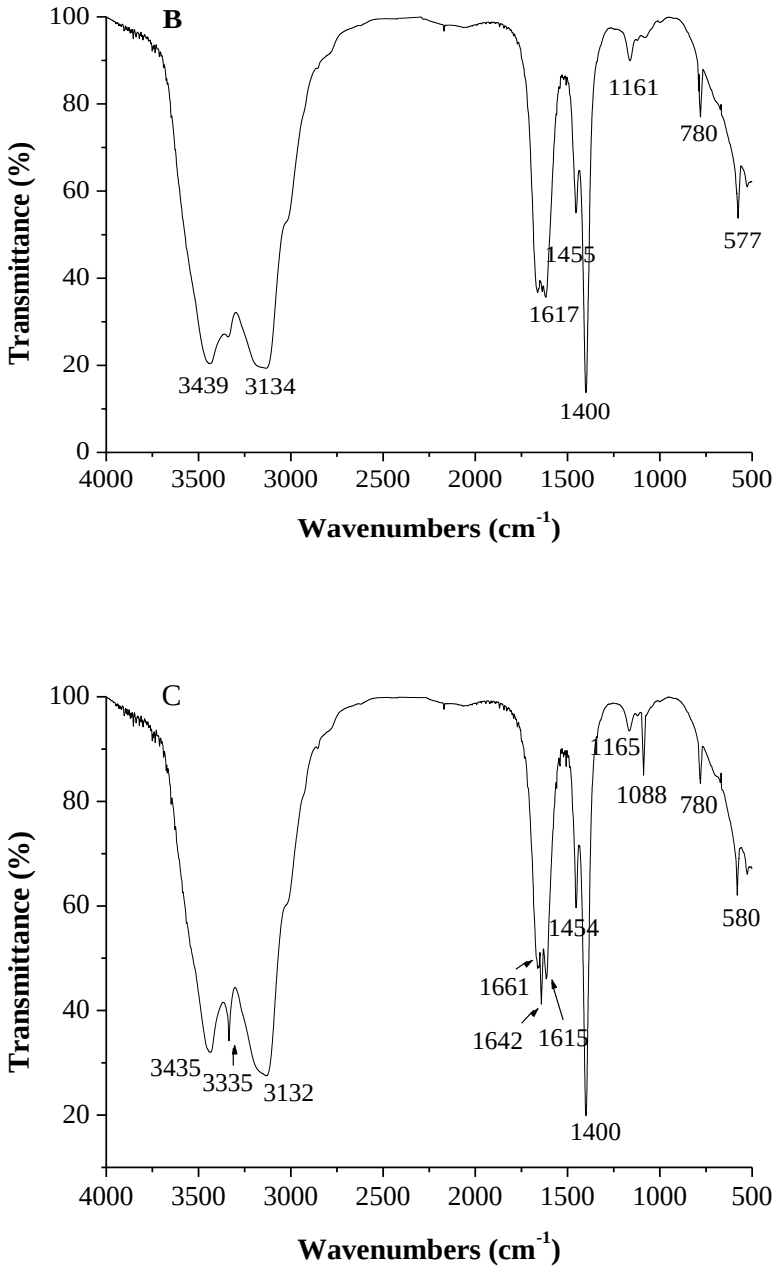

Fig. 2 FTIR spectra of (A) P*o*PD, (B) MWCNTs/P*o*PD composite and (C) MWCNTs/P*o*PD/PT composite.

The optimization of electropolymerized conditions

To obtain the best performance, several variables including the supporting electrolyte, ratio of

monomers, scan number and rate, removal of the template and incubation time were optimized by altering each variable in turn while keeping the others constant. All the optimization experiments were performed using LSV or CV.

Choice of supporting electrolyte. The choice of a suitable supporting electrolyte plays an important role in achieving the optimal electrochemical responses. In this work, different electrolytes including KCl, KNO_3, phosphate and the combination of each with different concentrations, were investigated as supporting electrolyte solutions. The 0.05 mol L^{-1} PBS containing 0.1 mol L^{-1} KCl rendered the MIP-MGCE best responses and therefore, was selected as supporting electrolyte.

Effect of the electropolymerization cycles and rate. The thickness of polymer membrane can easily be adjusted by controlling the number of cycles during the electropolymerization process. The response of MGCE during electropolymerization firstly decreased with increasing the number of cycles up to 20, and then kept almost stable above 20 cycles, which suggests a compact and scarcely conductive film is coated onto the MGCE surface progressively. The MIP-MGCE prepared at lower number of cycles demonstrated less sensitivity, probably due to the small number of recognition sites formed in the copolymer matrix. More cycles than needed could lead to more extensive electropolymerization, and consequently, to the formation of thicker sensing film with less accessible imprinted sites. Therefore, the polymerization cycles was chosen to be 20.

It has been reported that electropolymerization rate has an important effect on the morphology of polymer films. The MIP film electrodeposited slowly on the surface of the MGCE may be compact and smooth, while being rough and porous at a high growth rate. It was expected that the template would be firmly entrapped in the copolymer, and the template could hardly be removed when the scan rate is too low. It was found that the optimized scan rate was 50 mV s^{-1}.

Effect of extractant and incubation time. Before employing the as-prepared sensor for the subsequent analysis, the template entrapped in the polymer matrix must be removed to release the imprinted sites by an elution step. In this study, ethanol, ultra-pure water, ethanol–water, acetonitrile,

and acetonitrile–water was each applied to remove the template. The results show that ethanol–water (1:1, *v/v)* as the extractant can remove the template most quickly and completely. The elution process was developed by immersing the sensor into 20 mL extractant for 20 min, the electrode was then rinsed by doubly distilled water for several times.

The accumulation step is usually a simple and effective way of enhancing the sensitivity of the imprinted sensor. After the template was removed from the MIP film, the sensor was incubated in a 10 μmol L^{-1} PT solution for different time, then rinsed by doubly distilled water, dried under nitrogen in turn, and measure the peak current quantitatively. A stable response was obtained after immersion for 10 min, suggesting that the adsorption equilibrium was reached. Therefore, an incubation time of 10 min was selected whenever the measurement was made with the MIP sensor.

Electrochemical characterization of MIP-MGCE and NIP-MGCE

The CV response of an external redox couple is an effective and convenient tool to monitor the the different steps through the modification of the electrodes. The electrochemical behavior of the stepwise fabrication process was studied in 1.0 mmol L^{-1} $K_3[Fe(CN)_6]$ solution containing 0.1 mol L^{-1} KCl. $K_3[Fe(CN)_6]$ served as an electrochemical probe. As shown in Fig. 3, a couple of typical redox peaks of $K_3[Fe(CN)_6]$ appeared at bare GCE (curve a). When the surface was covered with MWCNTs-COOH layer, an increment of the redox peak current in the curve of the electrode was observed (curve b). The increase in the current of the CV for ferrycianide is due to the electrocatalytic effect of the MWCNTs-COOH and the increase in the electroactive area. When the imprinted film was electrosynthesized on the surface of MGCE, the peak current was not observed (curve c). It may be that the $K_3[Fe(CN)_6]$ could not pass through the layer of polymer to arrive at the surface of electrode. As shown in curve d, after the template removal, the redox current of $K_3[Fe(CN)_6]$ increased. It can be ascribed that upon the removal of the template, the formation of recognition sites or binding cavity made electron transfer possible and $K_3[Fe(CN)_6]$ could pass through the cavity and reach the surface of the electrode again. In contrast, for NIP-MGCE, there is almost no peak current

observed (curve e), which could be attributed to the fact that the NIP film, covering the surface of the MGCE, has polymerized in the absence of PT, so no cavities with binding sites were obtained. The results indicated that NIP-MGCE was unable to recognize PT.

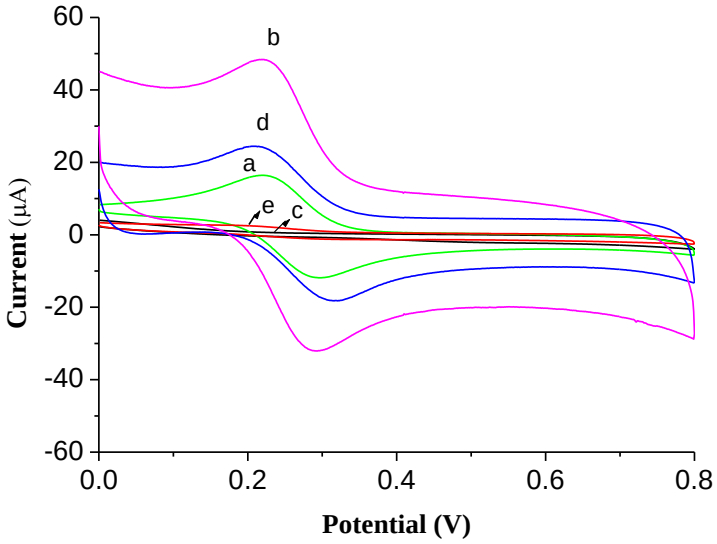

Fig. 3 Cyclic voltammograms of (a) bare GCE; (b) MGCE, (c) MIP-MGCE before PT removal, (d) MIP-MGCE and (e) NIP-MGCE. 1.0 mmol L^{-1} $K_3[Fe(CN)_6]$ in N_2-saturated PBS (0.05 mol L^{-1}, pH: 7.0) containing 0.1 mol L^{-1} KCl. Scan rate: 50 mV s^{-1}.

In order to confirm whether PT molecules had been embedded in the imprinted membranes, LSVs of the imprinted electrode before and after the removal of the imprinted PT molecules as well as the nonimprinted electrode were recorded in the N_2-saturated PBS containing KCl solution as supporting electrolyte respectively (Fig. 4). Before the removal of the imprinting PT molecules, a well-defined oxidation peak at +0.39 V was clearly recorded with MIP-MGCE (curve a). For MIP-GCE, only a small peak at +0.45 V recorded (curve b), suggesting a bad sensitivity to PT. However, for the nonimprinted electrode, no oxidation peak was observed (curve c). Since the electrochemical measurements were carried out in PT-free solutions, it is clearly confirmed that the strong oxidation peak was entirely due to the oxidation reaction of PT molecules embedded into the imprinted PT membranes. After immersing into 20 mL ethanol–water (1:1, *v/v)* for 10 min, there is no peak observed in the MIP-MGCE (curve d*)*, suggesting the PT molecules were totally removed from the

molecularly imprinted polymer film.

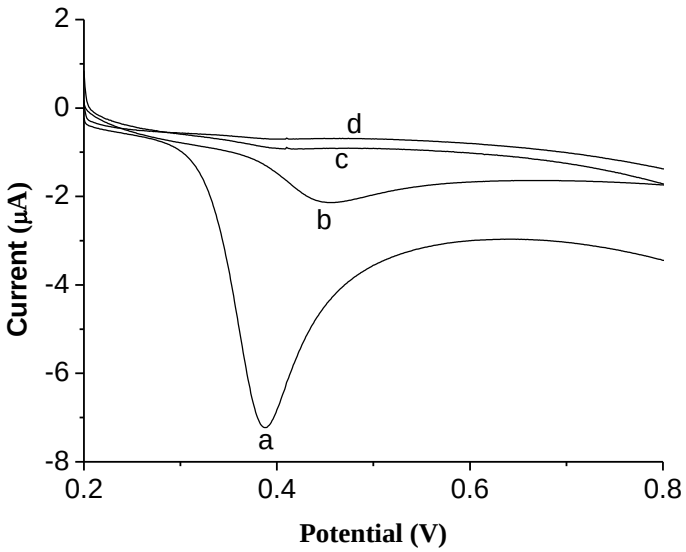

Fig. 4 LSVs of (a) MIP-MGCE, (b) MIP-GCE and (c) NIP-MGCE before the removal of PT; (d) LSVs of MIP-MGCE in the N_2-saturated PBS (0.05 mol L^{-1}, pH: 7.0) containing 0.1 mol L^{-1} KCl as supporting electrolyte. Scan rate: 50 mV s^{-1}.

Performance of the imprinted sensor

Selectivity of the MIP-MGCE. The selectivity of MIP-MGCE to PT was evaluated by testing its LSV responses in the presence of some possible interfering substances (their structures are shown in Fig. 5) including DA, PA, AA, AD and NAD, respectively.

At first we respectively studied the recognition ability of MIP-MGCE for PT and analytes with similar structures. Both MIP-MGCE and NIP-MGCE were respectively incubated for 10 min in 0.1 mol L^{-1} PBS including 10 μmol L^{-1} of different analytes, and then tested the LSV responses. The results are summarized in Fig. 6A (the original LSVs are shown in Fig. S3). It shows that the current value of MIP-MGCE toward PT is higher than that of the other analytes, whereas the adsorption capacities of NIP-MGCE are almost same. This good selectivity may come from a stronger affinity to PT which is attributed to the specific binding sites among the molecular imprinted polymer and the template. Secondly, the competitively selective property of PT by MIP-MGCE was evaluated by

calculating the peak current ratio (I_s/I_0), where I_s and I_0 were oxidation peak current of PT at 0.39 V in the present and absence of interfering substances (the original LSVs are shown in Fig. S4). As shown in Fig. 6B, a 10-fold excess of DA, PA, AA, AD and NAD over PT hardly causes the significant change of peak current of PT, in which peak current ratio only slightly varied from 0.92 to 1.07. These results indicate that MIP-MGCE showed higher recognition selectivity for PT. This may be explained by the fact that the delicate recognition sites of PT molecules in the imprinted membranes have the capability to recognize target molecules, allowing the detection of PT from a complex matrix without separation.

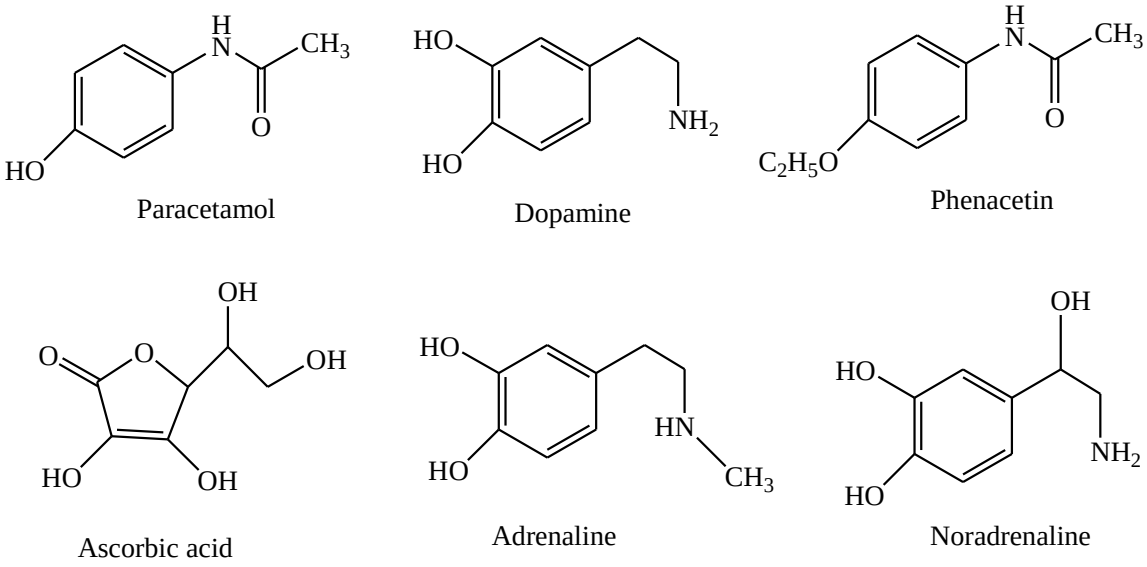

Fig. 5 The molecular structures of paracetamol (PT), dopamine (DA), phenacetin (PA), ascorbic acid (AA), adrenaline (AD), and noradrenaline (NAD).

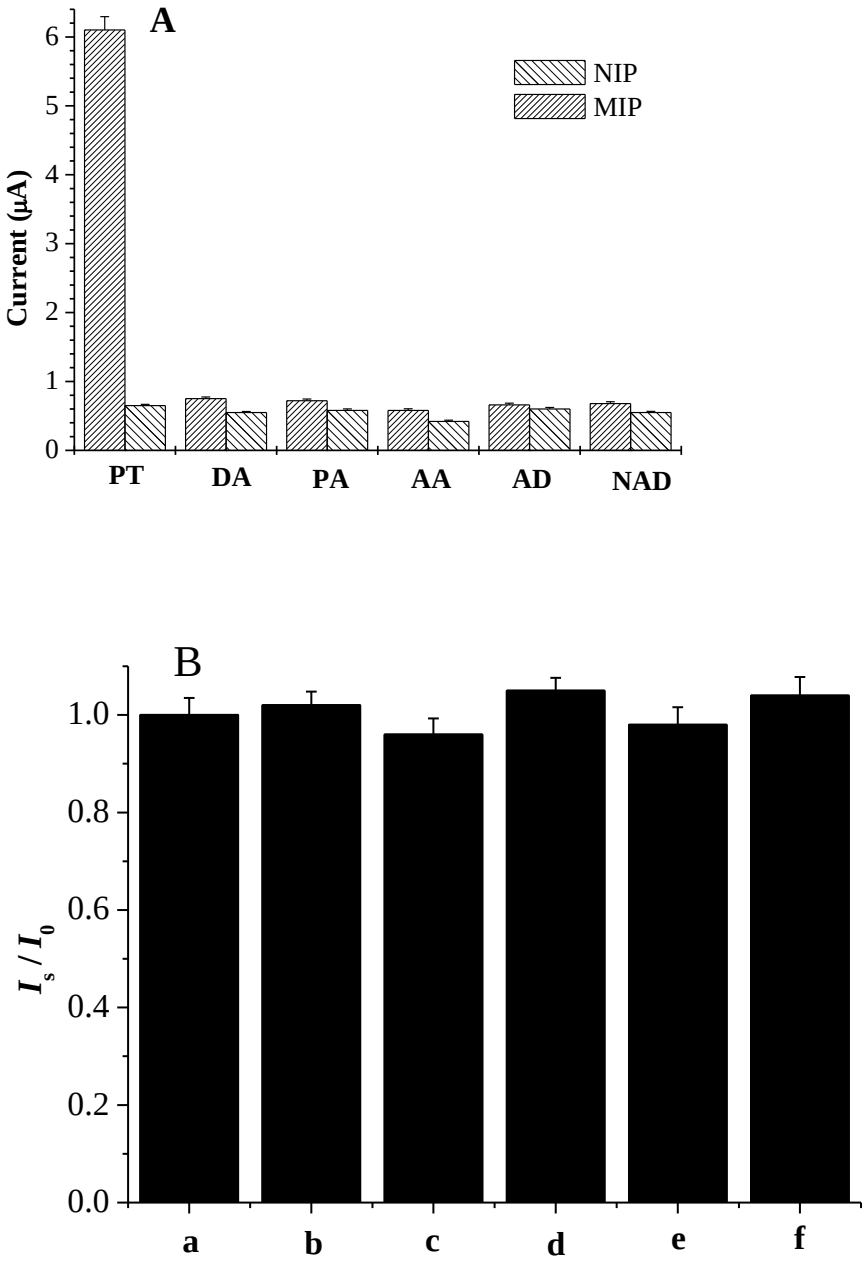

Fig. 6 (A) LSV peak currents of MIP-MGCE and NIP-MGCE to 10 μmol L^{-1} PT, 10 μmol L^{-1} DA, 10 μmol L^{-1} PA, 10 μmol L^{-1} AA, 10 μmol L^{-1}AD and 10 μmol L^{-1} NAD, respectively. (B) LSV peak current ratio (I_s/I_0) of MIP-MGCE to 1 μmol L^{-1} PT in the presence of 10 μM DA, PA, AA, AD and NAD, respectively. (a) 1 μmol L^{-1} PT; (b) 1 μmol L^{-1} PT and 10 μmol L^{-1} DA; (c) 1 μmol L^{-1} PT and 10 μmol L^{-1} PA; (d) 1 μmol L^{-1} PT and 10 μmol L^{-1} AA; (e) 1 μmol L^{-1} PT and 10 μmol L^{-1} AD; (f) 1 μmol L^{-1} PT and 10 μmol L^{-1} NAD. Preconcentration time is 10 min before measurement.

Calibration graph and detection limit. Fig. 7A displays the LSV responses of the imprinted

MIP-MGCE to PT after being incubated in PT solution. The sharp and well-defined peak current increased with PT concentration. A calibration curve between the peak current at 0.39 V and the PT concentration was exhibited in Fig. 7B. At higher concentration range, the peak currents tend to be stable, indicating that the imprinting sites were almost occupied by PT molecules. A linear relationship between the peak current and PT concentration was obtained covering the concentration range from 2.0×10^{-7} to 4.0×10^{-5} mol L^{-1}; the linear regression equation is I (μA) = – 0.00308 + 0.42235 c (μmol L^{-1}), with a correlation coefficient of 0.9934. The detection limit is calculated to be 5.0×10^{-8} mol L^{-1} based on the 3σ of the blank signals. The results obtained in this work were compared with some reported work in Table 1. It can be seen that our proposed method has lower limit of detection compare with that obtained on electropolymerized molecularly imprinted polypyrrole modified pencil graphite electrode[18], and that obtained on electrocopolymerized molecularly imprinted film modified carbon fiber microelectrodes.[35] The use of MWCNTs enhanced the sensitivity of detection and resulted in better LOD; however, the linear range in this work is not so wider, which may depend on the amount of recognition sites inside the molecular imprinted polymer film.

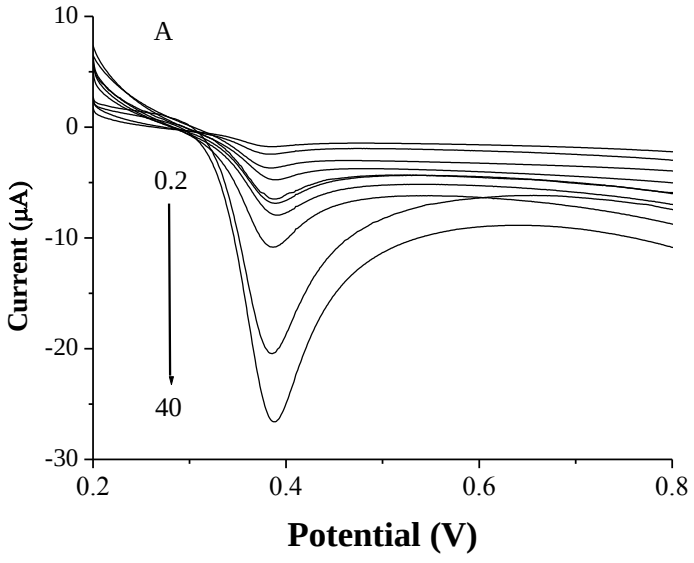

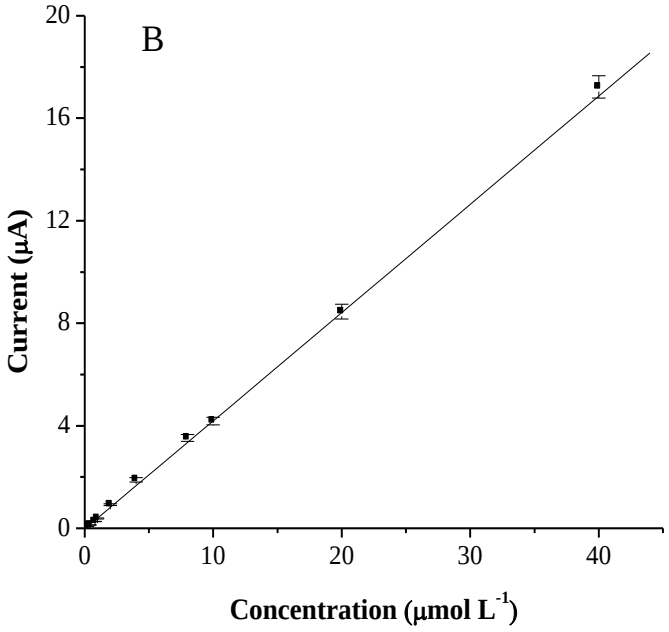

Fig. 7 (A), LSVs of increasing PT concentration in 0.05 mol L^{-1} PBS, pH: 7.0) containing 0.1 mol L^{-1} KCl. PT concentration was 0.2, 0.4, 0.8, 1, 2, 4, 8, 10, 20 and 40 μmol L^{-1}, respectively. Scan rate: 50 mV s^{-1}. (B), Calibration curve for PT. Data points and error bars represent the mean and ± 1 SD of 3 measurements, respectively.

Table 1. Comparison of the efficiency of different electrochemical sensors used in the analysis of PT.

Electrode	Modifer	Method	Linear range (mol L^{-1})	LOD (mol L^{-1})	pH	Ref.
GCE	MWCNTs/chitosan	DPV[a]	1.0×10^{-6} -1.45×10^{-4}	1.7×10^{-7}	7.0	10
CPE[b]	gold nanoparticles	DPV	5.0×10^{-8} –5.0×10^{-2}	7.7×10^{-9}	7.4	11
GCE	Nafion membrane doped with iron tetrapyridinoporphy-razine	AMP[c]	1.0×10^{-5}-5.0×10^{-2}	1.0×10^{-6}	3.6	12
GCE	$LaNi_{0.5}Ti_{0.5}O_3/CoFe_2O_4$ nanoparticle	LSV	5.0×10^{-7}-9.01×10^{-4}	1.9×10^{-7}	7.0	13
CPE	ethynylferrocene and NiO/MWCNT nanocomposite	SWV[d]	5.0×10^{-7}-6.0×10^{-4}	5.0×10^{-7}	6.0	14
pencil graphite	molecularly imprinted	DPV	5.0×10^{-6}-	7.9×10^{-7}	7.0	18

electrode	film		5.0×10^{-4}			
carbon fiber microelectrode	molecularly imprinted film	SWV	6.5×10^{-6}-2.0×10^{-3}	1.5×10^{-6}	7.0	35
GCE	Diglycolicacid	CV	2.0×10^{-8}-5.0×10^{-4}	6.7×10^{-9}	6.6	40
GCE	MWCNTs	DPV	5.0×10^{-7}-1.0×10^{-4}	4.2×10^{-7}	7.0	41
CPE	Ferrocene/ Carbon nanotube	LSV	4.7×10^{-7}-5.0×10^{-4}	2.1×10^{-7}	7.0	42
GCE	MWCNTs/molecularly imprinted film	LSV	2×10^{-7} – 4×10^{-5}	5.0×10^{-8}	7.0	This work

[a]Differential pulse voltammetry. [b]Carbon paste electrode. [c]Amperometric detection. [d]Square wave voltammetry.

Repeatability and stability of MIP-MGCE. The repeatability of the measurements was evaluated by measuring the LSV responses of 10 μmol L^{-1} PT at the same MIP-MGCE. The relative standard deviation (RSD) for seven successive determinations is about 2.5%. To investigate the repeatability of the MIPs sensor, the experiments were performed in10 μmol L^{-1} PT using different sensors. Five electrodes were prepared by using the same modification method. Then, the five electrodes were used to determine the same solution of PT (10 μmol L^{-1}). The calculated RSD were about 3.8% (n=7). The results showed that the proposed sensor had good repeatability. The regeneration experiment of the developed sensor was also performed. The regeneration procedure was as follows: in the experiment, after the detection, the electrodes were washed by ethanol–water (1:1, *v/v)* for 20 min to extract the templates. When the redox peak currents of these electrodes were the same as curve d in Fig. 2, the regeneration procedure was finished. It revealed that binding of PT to the "cavity" was reversible. The electrodes were allowed to dry and then were used to detect PT solution again. Afterwards, the electrodes were washed again and the next detection was processed likewise. The experimental results demonstrated the MIPs sensor could be regenerated very well.

The MIP-MGCE was stored under desiccated conditions at room temperature when not in use. The lifetime of the imprinted electrode was investigated by measuring the LSV responses of 10 μmol L^{-1} PT every 2 days. The response of the imprinted electrode decreased to 94% after storing for 10 days, and 85% of the original responses were retained after 20 days. Furthermore, detailed experiments reveal that, after the imprinted electrode was used at least 15 times with subsequent washing and

measuring operations, the response of PT at the MIP-MGCE hardly changed.

Application of the proposed method. The proposed method was utilized for the determination of PT in real samples including various tablets and syrup containing PT, human serum and human urine. Solution obtained by dissolution of PT tablets and syrup were subsequently diluted so that PT concentration lies in the range of calibration plot. LSVs were then recorded under exactly identical conditions that were employed for plotting calibration plot. Keeping dilution factor in consideration, it was found that PT concentration determined using this method is in good agreement with the manufacturers' stated contents (as shown in Table 2). The results of the sensor were compared with those obtained by capillary electrophoresis with electrochemical detection (CE-ED). When used for the detection of electroactive species in complex matrix, CE-ED has been considered to be a complementary technique to HPLC.[43] The apparatus and conditions for separation and determination of PT by CE-ED were described in detail in the literature.[44,45] When the proposed method was used in analysis of human serum and human urine, the recoveries varied from 94% to 105% (as shown in Table 3). Sensors based on MWCNTs modified GCE have been reported for the determination of PT in pharmaceutical preparations and biological fluids without sample pretreatments.[10,46] In combination with the specific selectivity of the molecular imprinting technique, the method proposed in this work may be applicable to detect PT for practical applications.

Table 2. Determination of PT concentration in pharmaceutical preparations using MIP-MGCE (n=3).

sample	Labeled content	Detected content	Detected by CE-ED	Added content	Found content	Recovery (%)	R.S.D. (%)
Tylenol syrup	100[a]	96[a]	105[a]	100[a]	191[a]	95	3.5
Tylenol Cold	325[b]	340[b]	345[b]	330[b]	683[b]	104	2.8
Contac NT	500[b]	510[b]	485[b]	500[b]	990[b]	96	3.6

[a]mg mL^{-1}

[b]mg $tablet^{-1}$

Table 3. Determination of PT in human serum and human urine with MIP-MGCE (n=3)

sample	Added content ($\mu mol\ L^{-1}$)	Found content ($\mu mol\ L^{-1}$)	Recovery (%)	R.S.D. (%)
1[a]	2.0	2.1	105	2.5
2[a]	20.0	19.2	96	3.2
3[b]	2.0	1.9	95	1.8
4[b]	20	20.8	94	2.8

[a]Human serum. [b]Human urine.

Conclusion

In this study, a MIP-MGCE formed by the CV electropolymerization of *o*PD film on MGCE in the presence of PT has been successfully fabricated. The optimized conditions for the MIPs film electropolymerization were also investigated. The prepared sensor displayed a good recognition capacity for template molecule in the presence of other structurally similar molecules. A linear relationship between the PT concentration and the current response was obtained with excellent reproducibility and a low detection limit of 5.0×10^{-8} mol L^{-1}. When the procedure was used for the determination of PT in samples of human serum, urine and some drugs, satisfactory results were obtained without the necessity of sample pretreatments and time-consuming extractions. The simple fabrication procedure, high stability, wide linear dynamic range and high sensitivity all suggests that the proposed sensor is an attractive candidate for practical applications.

Acknowledgements

The authors are grateful for the financial support provided by the Science Foundation of Quanzhou, Fujian province (grant No. 2012Z112).

References

1 R.M.D. Carvalho, R.S. Freire, S. Rath and L.T. Kubota, *J. Pharm. Biomed. Anal.*, 2004, **34**, 871.

2 R.T. Kachoosangi, G.G. Wildgoose and R.G. Compton, *Anal. Chim. Acta*, 2008, **618**, 54.

3 R.N. Goyal, V.K. Gupta, M. Oyama and N. Bachheti, *Electrochem. Commun.*, 2005, **7**, 803.

4 M. Li and L.H. Jing, *Electrochim. Acta*, 2007, **52**, 3250.

5 http://en.wikipedia.org/wiki/Paracetamol.

6 http://www.drugs.com/acetaminophen.html.

7 R.S. Andulescu, S. Mirel and R. Oprean, *J. Pharm. Biomed. Anal.*, 2000, **23**, 77.

8 M.S. Bloomfield. *Talanta*, 2002, **58**, 1301.

9 W. Peng, T. Li, H. Li and E. Wang, *Anal. Chim. Acta*,, 1994, **298**, 415.

10 A. Babaei, M. Afrasiabi and M. Babazadeh, *Electroanalysis*, 2010, **22**, 1743.

11. N. F. Atta, A. Galal, F. M. Abu-Attia and S. M. Azab. *J. Mater. Chem.*, 2011, **21**, 13015.

12**.** M. C. Q. Oliveira, M. R. V. Lanz, A. A. Tanakac and M. D. P. T. Sotomayor, *Anal. Methods*, 2010, **2**, 507.

13. D. X. Ye, Y. H. Xu, L. Q. Luo, Y. P. Ding, Y. L. Wang and X. J. Liu, J Solid State Electrochem., 2012, **16**, 1635.

14 M. R. Shahmiri, A. Bahari, H. Karimi-Maleh, R. Hosseinzadeh and N. Mirnia, *Sens. Actuators B, Chem.* 2013, **177**, 70.

15 D. Kumar and B. B. Prasad, *Sens. Actuators B, Chem.*, 2012, **171– 172**, 1141.

16 B. B. Prasad, A. Prasad and M.P.Tiwari, *Biosens. Bioelectron.*, 2013, **39**, 236.

17 Y. Fuchs, O. Soppera and K. Haupt, *Anal. Chim. Acta.*, 2012, **717**, 7.

18 L. Özcan and Y. Şahin, *Sens. Actuators B, Chem.*, 2007, **127**, 362.

19 C. Malitesta, I. Losito and P.G. Zambonin, *Anal. Chem.*, 1999, **71**, 1366.

20 F.L. Dickert, M. Tortschanoff, W.E. Bulst and G. Fischerauer, *Anal. Chem.*, 1999, **71**, 4559.

21 M. Riskin, R. Tel-Vered, T. Bourenko, E. Granot and I. Willner, *J. Am. Chem. Soc.*, 2008, **130**,

9726.

22 A. Gómez-Caballero, N. Unceta, M.A. Goicolea and R.J. Barrio, *Sens. Actuators B, Chem.*, 2008, **130**, 713.

23 E. Granot, R. Tel-Vered, O. Lioubashevski and I. Willner, *Adv. Funct. Mater*., 2008, 18, 478.

24 X. Kan, T. Liu, H. Zhou, C. Li and B. Fang, *Microchim. Acta*., 2010, **171**, 423.

25 S.P. Ozkorucuklu, Y. Sahin and G. Alsancak, *Sensors*, 2008, **8**, 8463.

26 C. Xie, S. Gao, Q. Guo and K. Xu, *Microchim. Acta*., 2008, **169**, 145.

27 Z. H. Zhang, Y. F. Hu, H. B. Zhang, L. J. Luo and S. Z. Yao, *Biosens. Bioelectron.*, 2010, **26**, 696.

28 X. W. Kan, Y. Zhao, Z. R. Geng, Z. L. Wang and J. J. Zhu, *J. Phys. Chem. C*, 2008, **112**, 4849.

29 I. Losito, F. Palmisano, P. G. Zambonin. *Anal. Chem.*, 2003, **75**, 4988

30 D. Chirizzi, C. Malitesta. *Sens. Actuators B*, 2011, **157**, 211

31 H. Peng, C.D. Liang, A.H. Zhou, Y.Y. Zhang, Q.J. Xie and S.Z. Yao, *Anal. Chim. Acta*., 2000, **423**, 221.

32 H.D. Li, H.M. Guan, H. Dai, Y.J. Tong, X.N. Zhao, W.J. Qi, S. Majeed and G.B Xu. Talanta, 2012, **99**, 811.

33 X.G.Li, M.R.Huang, W.Duan, and L.Yang, *Chem. Rev*. 2002, **102**, 2925.

34 M. Behzadi, E. Noroozian and M. Mirzaei, *Talanta*, 2013, **108**, 66.

35 A. Gómez-Caballero, M. A. Goicolea and R. J. Barrio, *Analyst*, 2005, **130**, 1012.

36 A. Prună and F. Brănzoi. *J. Polym. Res.*, 2012, **19**, 9879.

37. T. J. Durnick and S. C. Wait. *J Mol Spectrosc.*, 1972, **42**, 211.

38. W. H. Li, X. Y. Li, and N. T. Yu. *Chem. Phys. Lett.*, 2000, **327**, 153.

39 Y. Q. Duan, X. P. Luo, Y. Qin, H. H. Zhang, G. B. Sun, X. B. Sun, and Y. S. Yan. *J. Appl. Polym. Sci*., 2013, 129(5), 2882.

40 F. Xu, H. Y.Ru, L. X. Sun, Y. J. Zou, C. L. Jiao, T. Y. Wang, J.M. Zhang, Q. Zheng and H. Y. Zhou, *Biosensors and Bioelectronics*, 2012, **38**, 27.

41 J. B. Raoof, R. Ojani, M. Baghayeri and M. Amiri-Aref, *Anal. Methods*, 2012, **4**, 1579.

42 M. R. Akhgar, H. Beitollahi, M. Salari, H. Karimi-Maleh and H. Zamani. *Anal. Methods*, 2012, **4**,

259.

43 Y. Y. Peng, J. N. Ye, J. L. Kong. *J. Agric. Food Chem.*, 2005, **53**, 8141.

44. Y.Y. Peng, Q. C. Chu, F. H. Liu, J. N. Ye. *J. Agric. Food Chem.*, 2004, **52**, 153.

45. X. H. Ding, Q. C. Chu and J. N. Ye. *Chinese Journal of Instrumental Analysis*, 2002, **21**, 37.

46 A. Babaei, A. R. Taheri and M. Afrasiabi. *J. Braz. Chem. Soc.*, 2011, **22**, 1549.